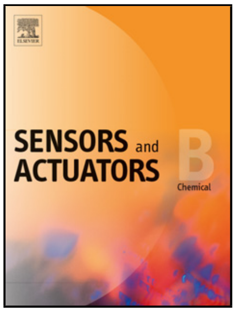

Title: ZnO/ZnAl$_2$O$_4$ Prepared by Calcination of ZnAl Layered Double Hydroxides for Ethanol Sensing

Author: <ce:author id="aut0005" biographyid="vt0005"> Mei-Yu Guan<ce:author id="aut0010" biographyid="vt0010"> Dong-Mei Xu<ce:author id="aut0015" biographyid="vt0015"> Yu-Fei Song<ce:author id="aut0020" biographyid="vt0020"> Ying Guo

PII: S0925-4005(13)00939-8
DOI: http://dx.doi.org/doi:10.1016/j.snb.2013.08.016
Reference: SNB 15825

To appear in: *Sensors and Actuators B*

Received date: 25-4-2013
Revised date: 15-7-2013
Accepted date: 4-8-2013

Please cite this article as: M.-Y. Guan, D.-M. Xu, Y.-F. Song, Y. Guo, ZnO/ZnAl$_2$O$_4$ Prepared by Calcination of ZnAl Layered Double Hydroxides for Ethanol Sensing, *Sensors and Actuators B: Chemical* (2013), http://dx.doi.org/10.1016/j.snb.2013.08.016

ZnO/$ZnAl_2O_4$ Prepared by Calcination of ZnAl Layered Double Hydroxides for Ethanol Sensing

Mei-Yu Guan, Dong-Mei Xu, Yu-Fei Song*, Ying Guo*

State Key Laboratory of Chemical Resource Engineering, Beijing University of Chemical Technology, Beijing 100029, P. R. China

*To whom correspondence should be addressed, Tel: (+86)-10-64412115, Email: songyufei@hotmail.com, guoying@mail.buct.edu.cn

Abstract: In this work, $ZnO/ZnAl_2O_4$ has been prepared by calcination of ZnAl layered double hydroxides (Zn_2Al-LDH), and the resulting products calcined at different temperatures have been characterized by powder X-ray diffraction (XRD), scanning electron microscopy (SEM), Fourier transform infrared spectroscopy (FT-IR), and ^{27}Al solid-state nuclear magnetic resonance (NMR). The gas sensing measurement indicates that the sample calcined at 1000°C shows much higher response to ethanol due to its better crystallinity of $ZnAl_2O_4$ than that calcined at 800°C or 600°C, respectively. In addition, the sample calcined at 1000°C exhibits fine repeatability and good selectivity for ethanol. It has been demonstrated that the $ZnAl_2O_4$ inside the calcined sample acts as a catalyst to accelerate the response and recovery behaviors in ethanol sensing.

Keywords: Layered double hydroxides, $ZnO/ZnAl_2O_4$, composite oxides, ethanol sensing

1. Introduction

Gas-sensing materials have been extensively studied over past two decades for detecting pollutants, toxic and combustible gases, which are closely related to environmental protection, public safety and human health. In particular, ethanol-sensing materials based on semiconductor oxides, like SnO_2 [1], Fe_2O_3 [2] , TiO_2 [3] and ZnO [4, 5], have been widely investigated due to high sensitivity, low cost and easy preparation [6]. However, the above mentioned semiconductor oxides often show the following disadvantages that largely restrict their application, such as high working temperature, poor long-term stability, and/or poor selectivity and so on. To solve these problems, much effort has been paid to improve the sensing properties by different approaches including the control of the operation temperature [7], the manipulation of the nano-structure [8] and surface modification [9], the design of multi-components composite oxides [10, 11] or the doping with a catalytic amount of component such as noble metal [12, 13]. Among these methods, the development of composite oxides shows great potential for tuning gas selectivity since the synergistic effects between different sensing components can improve the gas sensing properties. For instance, Kwon [14] reported that 4.0 wt% $A1_2O_3$ doped ZnO is highly sensitive and selective to trimethylamine gas; Yu [15] found that the ZnO/Zn_2SnO_4 exhibits higher sensing properties to CO and H_2 than single component of ZnO or Zn_2SnO_4. Bai et al. [16] synthesized ZnO/SnO_2 nanocomposite by reverse microemulsion and revealed that the nanocomposite shows superior thermal stability against grain growth and high sensitivity to NO_2. It is well-known that ZnO is an important semiconductor material, which has been applied in sensors due to their excellent chemical and thermal stability, non-toxicity, low cost, rapid response and fast recovery [17-21]. Meanwhile, Zinc aluminate ($ZnAl_2O_4$) with the spinel structure of AB_2O_4, has been widely used as catalyst [22] due to its high thermal stability, low acidity properties and relatively broad band gap. Recently, Yin [23] and Mortazavi [24] reported doping small amounts of various metals or metal oxides in the oxide-based gas sensitive materials can improve the gas sensitivity because of the additives' catalytic activity. As such, it is expected that the composite of $ZnO/ZnAl_2O_4$ would be promising for the enhancement of gas sensing properties considering the synergistic effects between each other and the catalytic property of $ZnAl_2O_4$.

Layered double hydroxides (LDHs) are a class of anionic layered clays with the general formula $[M^{2+}_{1-x}M^{3+}_{x}(OH)_2]^{x+}(A^{n-})_{x/n}\cdot mH_2O$, where M^{2+} and M^{3+} individually stands for various divalent and trivalent metal cations in the brucite-like host layers, and A^{n-} represents the interlayer guest anions in the hydrated interlayer galleries [25]. Over the past decades, based on the anion-exchange capability and compositional flexibility, LDHs have been applied in various fields as anion-exchangers [26], drug carriers [27], flame retardants [28] and hybrid pigments [29]. In addition, LDHs have been used for the fabrication of a large variety of composite oxides via calcined process. With LDHs as a single source precursor, the resulting composites show not only high specific surface areas, good stability against sintering and homogeneous dispersion between the elements, but also improved physio-chemical properties compared with the physical mixture of two different metal oxides [30, 31]. Therefore, in the current work, Zn_2Al-LDH was used as a single source to prepare the composite of $ZnO/ZnAl_2O_4$, and it turns out that $ZnO/ZnAl_2O_4$ shows high response, fine stability and good selectivity to ethanol.

Since calcination temperature has an important influence on the material's composition, crystallinity and structural stability, which would consequently affect the materials' gas response [32], the LDH precursor has been calcined at different temperatures (600, 800 and 1000°C) and the gas sensing behaviors have been investigated. As a result, the optimal calcination temperature to have the best ethanol sensing behavior is $1000^{o}C$ due to its high crystallinity of $ZnAl_2O_4$ and good catalytic property inside the calcined composite.

2. Experimental Section

2.1 Materials

The starting materials $Zn(NO_3)_2 \cdot 6H_2O$ (99.0% purity), $Al(NO_3)_3 \cdot 9H_2O$ (99.0% purity), and NaOH (96.0% purity) were purchased from Beijing Chemical Industry.

2.2 Preparation of LDH and the Calcined Products

Zn_2Al-LDH precursor was synthesized by using co-precipitation method [25] and followed by a hydrothermal process. $Zn(NO_3)_2 \cdot 6H_2O$ (5.95 g, 0.02 mol) and $Al(NO_3)_3 \cdot 9H_2O$ (3.75 g, 0.01 mol) were dissolved together in CO_2-free deionized water to make a mixed salt solution (100 mL). NaOH (3.2 g, 0.08 mol) was dissolved in CO_2-free deionized water to make a base solution (100 mL). The above two solutions were simultaneously added dropwise to a four-necked flask containing 30 mL of CO_2-free deionized water at 298K under constant stirring. The slurry was maintained in N_2 atmosphere at a constant pH of 6.5 ± 0.5. Afterwards, the resulting slurry was transferred into Teflon-lined autoclaves and aged at 100°C for 12 h. The resulting products were centrifuged, subsequently washed with CO_2-free deionized water and anhydrous ethanol for several times before being dried at 80°C in vacuum oven for 16 h. For the preparation of composite oxides, Zn_2Al-LDH precursor was placed in a muffle furnace and calcined in air at different temperatures of 600, 800 and 1000°C for 5 h at a heating rate of 10°C/min. The resulting products were named as ZSX-600, ZSX-800, and ZSX-1000, respectively.

2.3 Characterization

Powder X-ray diffraction (XRD) patterns of the samples were recorded in the 2θ range of 3–70° using a Rigaku XRD-6000 diffractometer under the following conditions: 40 kV, 30 mA, Cu-Kα radiation (λ =0.15418 nm). Thermogravimetric and differential thermal analysis (TG-DTA) were carried out in air on a PCT-1A thermal analysis system produced locally. Elemental analysis for metal ions in LDHs was performed using a Shimadzu ICPS-7500 inductively coupled plasma emission spectrometer (ICP-ES) and the C, H, N contents in LDH were determined by Elementary Vario EL analyzer. Fourier transform infrared (FTIR) spectra were recorded in the range of 4000 to 400 cm^{-1} on a Bruker Vector-22 Fourier transform infrared spectrometer using the KBr pellet technique (1 mg of sample in 100 mg of KBr). Scanning electron microscopy (SEM) images were obtained using a Zeiss SUPRA 55 at 20 kV, with the surface of the samples coated with a thin platinum layer to avoid a charging effect. ^{27}Al nuclear magnetic resonance (NMR) spectra were recorded on a Bruker Avance III 400WB spectrometer. The spectra were measured using a 4 mm rotor at a spinning rate of 10 kHz, and accumulation of 800 scans. The chemical shifts were referenced to aluminum nitrate solution at 0.0 ppm.

2.4 Gas Sensing Measurements

Gas sensing tests were conducted on a measuring system of chemical gas sensing-8 (CGS-8) in ELITE TECH. The sensor device we used is a custom-built one, which is widely used for gas sensing test [33, 34]. Two gold electrodes are printed on the ceramic tube with a gap of about 1 mm, and four Pt wires are positioned on the gold electrodes. A small Ni - Cr alloy coil is placed through the tube as a heater, which providing the working temperature of the gas sensor. By varying the heating current, the working temperature of the sensors can be adjusted.

The sensor was fabricated in a similar way to that reported [33], the calcined product was ground in an agate mortar with a little water to form a paste. The paste was coated onto the above alumina ceramic tubes before being dried for a few minutes. Afterwards, the sensor was aged at 80 mA for 24 h in air to improve its stability. The optical micrographs of a blank and a sample sensor are shown in Figure 1.

The gas responses were measured by observing the sensors' resistance change in different gases. The gas response value is designated as $S = R_a/R_g$, where R_a is the sensor resistance in air (base resistance) and R_g is that in the target gas. The time taken by the sensor resistance to change from R_a to R_a - 90% × (R_a-R_g) is defined as response time after the target gas being introduced to the sensor, and the time taken from R_g to $R_g + 90\% \times (R_a - R_g)$ is defined as recovery time after the ambience being replaced by air.

3. Results and discussion

3.1 Characterization of LDHs and the Calcined Products

The XRD pattern of the Zn_2Al-LDH precursor exhibits typical characteristics of LDH phase (Figure S1). Elemental analysis, ICP and TG-DTA (Table S1 and Figure S2) confirm the structural formula of the synthesized LDH is $Zn_{0.67}Al_{0.33}(OH)_{2.11}(NO_3)_{0.22}\cdot 0.5H_2O$. As shown in Figure 2, the lamellar structure collapses after calcination. It is noted that the LDH precursor transforms into the mixture of wurzite-structured ZnO and spinel-structured $ZnAl_2O_4$ [35] at different calcined temperatures. The relative intensities of $ZnAl_2O_4$-related signals grow stronger and sharper with the increase of calcination temperature, indicating the better crystallinity of the spinel-structured $ZnAl_2O_4$ at higher temperatures.

Figure 3 shows the FT-IR spectra of the calcined products. Compared with Zn_2Al -LDH precursor (Figure S3), the bands at 3500 cm^{-1} and 1384 cm^{-1} in Zn_2Al-LDH are not present in the corresponding calcined samples, which are attributed to the removal of water molecules and the decomposition of the NO_3^- groups in the LDH interlayer. In the three calcined samples, the bands at 499 cm^{-1}, 553 cm^{-1} and 662 cm^{-1} are related to Al–O bonds in the $ZnAl_2O_4$ phase [35]. The bands at 662, 553 cm^{-1} are assigned to the stretching modes of AlO_6 octahedral units, and the band observed at 494 cm^{-1} is due to the bending mode of AlO_6 octahedral units [36]. Therefore, FT-IR spectra provide further support for the formation of $ZnAl_2O_4$ spinel during calcination, which is in good agreement with XRD results.

SEM of Zn_2Al-LDH and the calcined samples are shown in Figure 4. It can be seen that the Zn_2Al-LDH precursor with lamellar structure transforms into small pieces with similar shapes after calcination. There are a number of blocks randomly dispersed on the surface of ZSX-600 in the presence of Zn and Al elements from the Energy Dispersive Spectroscopy (Figure S4). SEM images of ZSX-800 and ZSX-1000 show more pores on the surface and less blocks than those of ZSX-600, which might be due to the release of interlayer water and the dehydroxylation of the metal hydroxide layers during calcination.

Similar to the XRD results, the layers of Zn_2Al-LDH are destroyed and $ZnAl_2O_4$ spinel phases are formed after calcinations, which could be proved by the ^{27}Al NMR spectra (Figure 5). As can be seen from the ^{27}Al NMR spectra, one single and intensive resonance of LDHs (Figure 5a) is centered at about 15 ppm for octahedral coordination of Al^{3+} ions, which indicates a single coordination environment in Zn_2Al-LDH precursor. As mentioned above, the $ZnAl_2O_4$ spinel phases form during calcination. It is worth noting that the normal zinc aluminate spinel with a general formula of XY_2O_4 forms with a face centered cubic structure and two lattice sites available for cation occupancy, where X^{2+} and Y^{3+} cations occupy the tetrahedral sites and octahedral sites, respectively. The inverse spinel has a general formula of $Y[XY]O_4$, in which X^{2+} and half of the Y^{3+} cations occupy the octahedral sites, and the other half of the Y^{3+} cations occupy the tetrahedral sites. In our work, two main resonances appear at ~ 10 ppm and ~ 70 ppm in three calcined samples (Figure 5b-5d).

The signal at ~ 10 ppm are characteristic of Al^{3+} ions occupying the AlO_6 sites, whereas the signal at ~ 70 ppm indicates some Al^{3+} occupy the AlO_4 sites [37, 38]. As such, the spinel phase should belong to the inverse spinel structure. The presence of two peaks (a doublet) at ~ 10 ppm for the samples calcined at 800°C and 1000°C can be resulted from the second order splitting by the nuclear-quadrupole interaction on the central transition band [39], which indicates imporoved crystallinity nature of $ZnAl_2O_4$ calcined at higher temperatures.

3.2 Ethanol Sensing Measurements

For n-type semiconductors, the gas detection processes are based on surface reaction between the adsorbed oxygen molecules and the gas to be detected [12, 40]. In the current work, the composite of $ZnO/ZnAl_2O_4$ is a typical n-type semiconductor. When the sensors are exposed in air, oxygen molecules are adsorbed onto the surface of the materials to form O_2^-, O^-, O^{2-} ions by capturing electrons from the conduction band of the composite [41]. Then, the carrier concentration of conduction band decreases and the electronic depletion layers are formed. As a result, the electronic conduction decreases [42]. Once the reducing ethanol gas is introduced and reacts with the adsorbed negatively charged oxygen, the trapped electrons are given back to the conduction band of the composite oxides, leading to the increase of the carrier concentration of the conduction band. Accordingly, the resistance of sensors decreases at the atmosphere of the detected gas, and the value of R_a/R_g increases. When the sensors are exposed back to air, the above process of absorbing oxygen repeats again, which leads to the decrease of the R_a/R_g. Obviously, for n-type semiconductor, the higher the R_a/R_g is, the higher the gas response is.

It is known that each gas sensing materials has an optimal operation temperature [43]. Figure 6 shows the sensor responses to 500 ppm ethanol for ZSX-600, ZSX-800 and ZSX-1000 at the operation temperature range of 170-320°C. Taking ZSX-1000 as an example, we can find that ethanol response is increasing gradually with the increase of operation temperature until the maximum R_a/R_g could be achieved at 240°C. With the increase of the operation temperature, the chemical adsorption of oxygen molecules gradually dominates, resulting in the high concentration of adsorbed oxygen species on the material's surface until the gas response reaches the maximum. Further increase of the operation temperature (above 240°C), the concentration of negatively charged oxygen species descends and the gas response decreases accordingly. Similarly, the optimal operation temperature of ZSX-800 and ZSX-600 are at 220°C and 210°C, respectively.

The calcination temperature of LDHs would influence the resulting sample's structure, morphology, composition and thereby the products' properties, such as the gas sensing behaviors etc. It has been demonstrated that the ethanol response of ZSX-1000 is the highest in the range of 200～300°C, which is 88 (R_a/R_g) at its optimal operation temperature (240°C) and is about 16 times of ZSX-600's ethanol response and 3.67 times of ZSX-800's ethanol response. The above results indicate that the calcination temperature has a great influence on ethanol response. It could be explained as follows: for ZSX-1000, it has a better crystallinity than ZSX-600 and ZSX-800, which can be observed from the XRD patterns and solid state NMR spectra.

The spinel $ZnAl_2O_4$ inside the composite helps to accelerate the ethanol response due to the good crystallinity of $ZnAl_2O_4$. Therefore, it can be concluded that the higher the calcination temperature is, the better the ethanol response is.

As shown in Figure 7, the gas responses increase linearly with the increase of ethanol concentrations. At the operating temperature of 240°C, the gas responses (R_a/R_g) of ZSX-600, ZSX-800 and ZSX-1000 to 100 ppm ethanol are 1.3, 12.5 and 40.0, respectively. Additionally, it can be seen that the response of the sample calcined at 1000°C increases drastically with the increase of ethanol concentration, while the sample caicined at 800°C and 600°C show slow increase in response.

Figure 8 shows the changes in electrical resistance for the three calcined samples. It can be seen that the response and recovery time of ZSX-1000 to 500 ppm ethanol at 240°C are about 1 s and 20 s, respectively, which are the shortest ones among the three samples. This is consistent with the fact that the better crystallinity of $ZnAl_2O_4$ inside ZSX-1000 plays an active catalytic effect on ethanol response. Moreover, the porous-like structure of ZSX-1000 probably not only provides enough domains to reduce space hindrance induced by the gas adsorption, but also increases its inner surface for speeding up the gas diffusion [44]. Therefore, the effect of porous structure might also help to improve the gas adsorption and speed up response.

Due to ZSX-1000 has a relatively high response to ethanol with short response/recovery time in comparison with ZSX-600 and ZSX-800, further gas sensing measurements have been focused on ZSX-1000 at its optimal operation temperature of 240°C. To exploit the repeatability of ZSX-1000 for gas sensing, its response and recovery behaviors upon exposure to ethanol vapor with different concentration of 100, 500, 1000 ppm have been checked at the working temperature of 240°C. As shown in Figure 9, the electrical resistance of ZSX-1000 undergoes a large decline upon the injection of ethanol and then rises to their initial value after the sensors being exposed to air. At the concentration of 1000 ppm, ZSX-1000 exhibits the lowest electrical resistance. The whole response and recovery process indicates ZSX-1000 shows a good reproducibility and stabilities. Moreover, the selectivity of gas sensor is also an important factor in view of practical application. For ZSX-1000, its gas responses to a series of typical volatile organic compounds were tested at the operating temperature of 240^{o}C as shown in Figure 10. We can find ZSX-1000 exhibits very high response to ethanol but less response to acetone and very low responses to ethanediol, benzene, NH_3 and formamide with the same concentration of 500 ppm, which demonstrates ZSX-1000 exhibits highly selective detection of ethanol. The above ZSX-1000 has a potential application in gas sensing field.

4. Conclusions

The present paper reports for the first time the ethanol sensing behavior of $ZnO/ZnAl_2O_4$ prepared from a single precursor of Zn_2Al-LDH via a calcination approach. Besides the synergistic effects between ZnO and $ZnAl_2O_4$, the calcination temperature, the crystallinity for $ZnAl_2O_{4,}$ and the porous-like morphologies along with the catalytic characteristic of $ZnAl_2O_4$ play vital role for the improvement of gas response. The sample calcined at 1000^{o}C performs impressive ethanol sensing behaviors, which are high response, good repeatability, favorable selectivity as well as fast response/recovery process. The present finding clearly demonstrates that the composite of ZnO/$ZnAl_2O_4$ would be an effective candidate for future gas sensing applications.

Acknowledgments

This work was supported by the National Natural Science Foundation of China (21001014, 21222104, 21076020), Beijing Natural Science Foundation (2113049), the program for New Century Excellent Talents of the Ministry of Education of China (NCET-09-0201), and Program for Changjiang Scholars and Innovative Research Team in University (IRT1205).

References:

[1] T. Waitz, B. Becker, T. Wagner, T. Sauerwald, C.D. Kohl, M. Tiemann, Ordered nanoporous SnO_2 gas sensors with high thermal stability, Sens. Actuators B: Chem. 150 (2010) 788-793.

[2] Z. Jing, Y. Wang, S. Wu, Preparation and gas sensing properties of pure and doped γ-Fe_2O_3 by an anhydrous solvent method, Sens. Actuators B: Chem. 113 (2006) 177-181.

[3] I.D. Kim, A. Rothschild, B.H. Lee, D.Y. Kim, S.M. Jo, H.L. Tuller, Ultrasensitive chemiresistors based on electrospun TiO_2 nanofibers, Nano Lett. 6 (2006) 2009-2013.

[4] Y. Liu, J. Dong, P.J. Hesketh, M. Liu, Synthesis and gas sensing properties of ZnO single crystal flakes, J. Mater. Chem. 15 (2005) 2316-2320.

[5] L.Chen , Z. Liu , S. Bai , K. Zhang ,D. Li, A. Chen , et al., Synthesis of 1-dimensional ZnO and its sensing property for CO, Sens. Actuators B: Chem. 143 (2010) 620-628.

[6] Z. Chen, M. Cao, C. Hu, Novel Zn_2SnO_4 hierarchical nanostructures and their gas sensing properties toward ethanol, J. Phys. Chem C. 115 (2011) 5522-5529.

[7] S. Chakraborty, A. Sen, H.S. Maiti, Selective detection of methane and butane by temperature modulation in iron doped tin oxide sensors, Sens. Actuators B: Chem. 115 (2006) 610-613.

[8] S. Bai, L. Chen, D. Li , W. Yang , P. Yang, Z. Liu , et al., Different morphologies of ZnO nanorods and their sensing property, Sens. Actuators B: Chem. 146 (2010) 129-137.

[9] X. Liu, J. Zhang, X. Guo, S. Wu, S. Wang, Enhanced sensor response of Ni-doped SnO_2 hollow spheres, Sens. Actuators B: Chem. 152 (2011) 162-167.

[10] S. Bai, D. Li, D. Han, R. Luo, A. Chen, C.L. Chung, Preparation, characterization of WO_3–SnO_2 nanocomposites and their sensing properties for NO_2, Sens. Actuators B: Chem. 150 (2010) 749-755.

[11] C.Y. Lin, Y.Y. Fang, C.W. Lin, J.J. Tunney, K.C. Ho, Fabrication of NO_x gas sensors using In_2O_3–ZnO composite films, Sens. Actuators B: Chem. 146 (2010) 28-34.

[12] J.K. Choi, I.S. Hwang, S.J. Kim, J.S. Park, S.S. Park, U. Jeong, et al., Design of selective gas sensors using electrospun Pd-doped SnO_2 hollow nanofibers, Sens. Actuators B: Chem. 150 (2010) 191-199.

[13] T.D. Senguttuvan, V. Srivastava, J.S. Tawal, M. Mishra, S. Srivastava, K. Jain, Gas sensing properties of nanocrystalline tungsten oxide synthesized by acid precipitation method, Sens. Actuators B: Chem. 150 (2010) 384-388.

[14] S.H. Park, J.Y. Ryu, H.H. Choi, T.H. Kwon, Zinc oxide thin film doped with Al_2O_3, TiO_2 and V_2O_5 as sensitive sensor for trimethylamine gas, Sens. Actuators B: Chem. 46 (1998) 75-79.

[15] J.H. Yu, G.M. Choi, Current–voltage characteristics and selective CO detection of Zn_2SnO_4 and ZnO/Zn_2SnO_4, SnO_2/Zn_2SnO_4 layered-type sensors, Sens. Actuators B: Chem. 72 (2001) 141-148.

[16]L. Chen, S. Bai, G. Zhou, D. Li, A. Chen, C. L. Chung, Synthesis of ZnO–SnO_2 nanocomposites by microemulsion and sensing properties for NO_2, Sens. Actuators B: Chem. 134 (2008) 360-366.

[17] J.F. Chang, H.H. Kuo, I.C. Leu, M.H. Hon, The effects of thickness and operation temperature on ZnO:Al thin film CO gas sensor, Sens. Actuators B: Chem. 84 (2002) 258-264.

[18] A. Kolmakov, Y. Zhang, G. Cheng, M. Moskovits, Detection of CO and O_2 using tin oxide nanowire sensors, Adv. Mater. 15 (2003) 997-1000.

[19] Q. Yuan, Y. Zhao, L. Li, T. Wang, Ab initio study of ZnO-based gas-sensing mechanisms: surface reconstruction and charge transfer, J. Phys. Chem C. 113 (2009) 6107-6113.

[20] B. Claflin, D.C. Look, S.J. Park, G. Cantwell, Persistent n-type photoconductivity in p-type ZnO, J. Cryst. Growth. 287 (2006) 16-22.

[21] G. Korotcenkov, Gas response control through structural and chemical modification of metal oxide films: state of the art and approaches, Sens. Actuators B: Chem. 107 (2005) 209-232.

[22] X. Wang, M. Zhang, H. Ding, H. Li, Z. Sun, Low-voltage cathodoluminescence properties of green-emitting $ZnAl_2O_4:Mn^{2+}$ nanophosphors for field emission display, J. Alloys Compd. 509 (2011) 6317-6320.

[23] C. Wang, L. Yin, L. Zhang, D. Xiang, R. Gao, Metal oxide gas sensors: sensitivity and influencing factors, Senors10 (2010) 2088-2106.

[24] H.M. Aliha, A.A. Khodadadi, Y. Mortazavi, The sensing behaviour of metal oxides (ZnO, CuO and Sm_2O_3) doped-SnO_2 for detection of low concentrations of chlorinated volatile organic compounds, Sens. Actuators B: Chem. 181 (2013) 637-643.

[25] K. Morimoto, K. Tamura, N. Iyi, J. Ye, H. Yamada, Adsorption and photodegradation properties of anionic dyes by layered double hydroxides, J. Phys. Chem. Solids. 72 (2011) 1037-1045.

[26] Y. Guo, D. Li, C. Hu, Y. Wang, E. Wang, Layered double hydroxides pillared by tungsten polyoxometalates: synthesis and photocatalytic activity, Int. J. Inorg. Mater. 3 (2001) 347-355.

[27] P. Gunawan, R. Xu, Direct assembly of anisotropic layered double hydroxide (LDH) nanocrystals on spherical template for fabrication of Drug-LDH hollow nanospheres, Chem. Mater. 21 (2009) 781-783.

[28] B. Du, Z. Guo, Z. Fang, Effects of organo-clay and sodium dodecyl sulfonate intercalated layered double hydroxide on thermal and flame behaviour of intumescent flame retarded polypropylene, Polym. Degrad. Stab. 94 (2009) 1979-1985.

[29] L. Latterini, M. Nocchetti, G.G. Aloisi, U. Costantino, F. Elisei, Organized chromophores in layered inorganic matrices, Inorg. Chim. Acta. 360 (2007) 728-740.

[30] X. Zhao, F. Zhang, S. Xu, D.G. Evans, X. Duan, From layered double hydroxides to ZnO-based mixed metal oxides by thermal decomposition: transformation mechanism and uv-blocking properties of the product, Chem. Mater. 22 (2010) 3933-3942.

[31] Q. Xu, D. Xu, M. Guan, Y. Guo, Q. Qi, G. Li, $ZnO/Al_2O_3/CeO_2$ composite with enhanced gas sensing performance, Sens. Actuators B: Chem. 177 (2013) 1134-1141.

[32] J.T. McCue, J.Y. Ying, $SnO_2-In_2O_3$ nanocomposites as semiconductor gas sensors for CO and NO_x detection, Chem. Mater. 19 (2007) 1009-1015.

[33] F. Song, H. Su, J. Han, W.M. Lau, W.J. Moon, D. Zhang, bioinspired hierarchical tin oxide scaffolds for enhanced gas sensing properties, J. Phys. Chem C. 116 (2012) 10274-10281.

[34] J. Zhang, S. Wang, Y. Wang, M. Xu, H. Xia, S. Zhang, et al., Facile synthesis of highly ethanol-sensitive SnO_2 nanoparticles, Sens. Actuators B: Chem. 139 (2009) 369-374.

[35] A.A.A. Ahmed, Z.A. Talib, M.Z.b. Hussein, A. Zakaria, Improvement of the crystallinity and photocatalytic property of zinc oxide as calcination product of Zn–Al layered double hydroxide, J. Alloys Compd. 539 (2012) 154-160.

[36] A.A. Da Silva, A.D.S. Gonçalves, M.R. Davolos, Characterization of nanosized $ZnAl_2O_4$ spinel synthesized by the sol–gel method, J. Sol-Gel Sci. Technol. 49 (2009) 101-105.

[37] N.J. van der Laag, M.D. Snel, P.C.M.M. Magusin, G. de With, Structural, elastic, thermophysical and dielectric properties of zinc aluminate (ZnAlO), J. Eur. Ceram. Soc. 24 (2004) 2417-2424.

[38] A. Vyalikh, D. Massiot, U. Scheler, Structural characterisation of aluminium layered double hydroxides by ^{27}Al solid-state NMR, Solid State Nucl. Magn. Reson. 36 (2009) 19-23.

[39] X. Duan, D. Yuan, F. Yu, Cation distribution in Co-doped $ZnAl_2O_4$ nanoparticles studied by X-ray photoelectron spectroscopy and ^{27}Al solid-state NMR spectroscopy, Inorg. Chem. 50 (2011)

5460-5467.

[40] D.R. Patil, L.A. Patil, D.P. Amalnerkar, Ethanol gas sensing properties of Al_2O_3-doped ZnO thick film resistors, Bull. Mater. Sci. 30 (2007) 553-559.

[41] J. Xu, J. Han, Y. Zhang, Y. Sun, B. Xie, Studies on alcohol sensing mechanism of ZnO based gas sensors, Sens. Actuators B: Chem. 132 (2008) 334-339.

[42] C.M. Ghimbeu, J. Schoonman, M. Lumbreras, M. Siadat, Electrostatic spray deposited zinc oxide films for gas sensor applications, Appl. Surf. Sci. 253 (2007) 7483-7489.

[43] T. Zhang, F. Gu, D. Han, Z. Wang, G. Guo, Synthesis, characterization and alcohol-sensing properties of rare earth doped In_2O_3 hollow spheres, Sens. Actuators B: Chem. 177 (2013) 1180-1188.

[44] K.I. Choi, H.R. Kim, J.H. Lee, Enhanced CO sensing characteristics of hierarchical and hollow In_2O_3 microspheres, Sens. Actuators B: Chem. 138 (2009) 497-503.

Vitae

Mei-Yu Guan is a master student in Dr. Guo's group, in the College of Science, Beijing University of Chemical Technology, China. Her project is focusing on the preparation and characterization of composite oxides for gas sensing application.

Dong-Mei Xu is a master student in Dr. Guo's group, in the College of Science, Beijing University of Chemical Technology, and she is working on the preparation and characterization of gas sensing materials for room temperature application.

Dr. Ying Guo is a Lecture at State Key Laboratory of Chemical Resource Engineering, Beijing University of Chemical Technology, China. Her work mainly focuses on the inorganic/organic nanocomposites in gas sensing, supramolecular assemblies based on intercalated chemistry etc.

Dr. Yu-Fei Song is a Professor of Chemistry at State Key Laboratory of Chemical Resource Engineering, Beijing University of Chemical Technology, China. His research interests include inorganic supramolecular assemblies, polyoxometalate catalysis, functional inorganic/organic hybrids etc.

Highlights

- $ZnO/ZnAl_2O_4$ was prepared from Zn_2Al-LDH precursor via a calcination method.
- $ZnO/ZnAl_2O_4$ prepared at 1000°C shows the best ethanol-sensing performance.
- $ZnAl_2O_4$ inside the sensing material plays a critical role in ethanol sensing.

Captions of Figures

Figure 1. Photographs of blank sensor and sample sensor.

Figure 2. Powder XRD patterns for (a) ZSX-600, (b) ZSX-800 and (c) ZSX-1000.

Figure 3. FTIR Spectra for (a) ZSX-600, (b) ZSX-800 and (c) ZSX-1000.

Figure 4. SEM images of (a) Zn_2Al-LDH, (b) ZSX-600, (c) ZSX-800 and (d) ZSX-1000.

Figure 5. The ^{27}Al NMR spectra for (a) Zn_2Al-LDH, (b) ZSX-600, (c) ZSX-800 and (d) ZSX-1000.

Figure 6. Responses of (a) ZSX-600, (b) ZSX-800 and (c) ZSX-1000 to 500 ppm ethanol versus operation temperatures.

Figure 7. Responses of gas sensing materials versus ethanol concentrations at 240°C for (a) ZSX-600, (b) ZSX-800 and (c) ZSX-1000).

Figure 8. Response/recovery curves of (a) ZSX-600, (b) ZSX-800 and(c) ZSX-1000 to 500 ppm ethanol at 240°C.

Figure 9. Repeatability of ZSX-1000 to 100 ppm, 500 ppm, 1000 ppm ethanol at 240°C.

Figure 10. Selectivity of ZSX-1000 to 500 ppm vapors at 240°C.

Figure(s)

blank sensor

sample sensor

Figure(s)

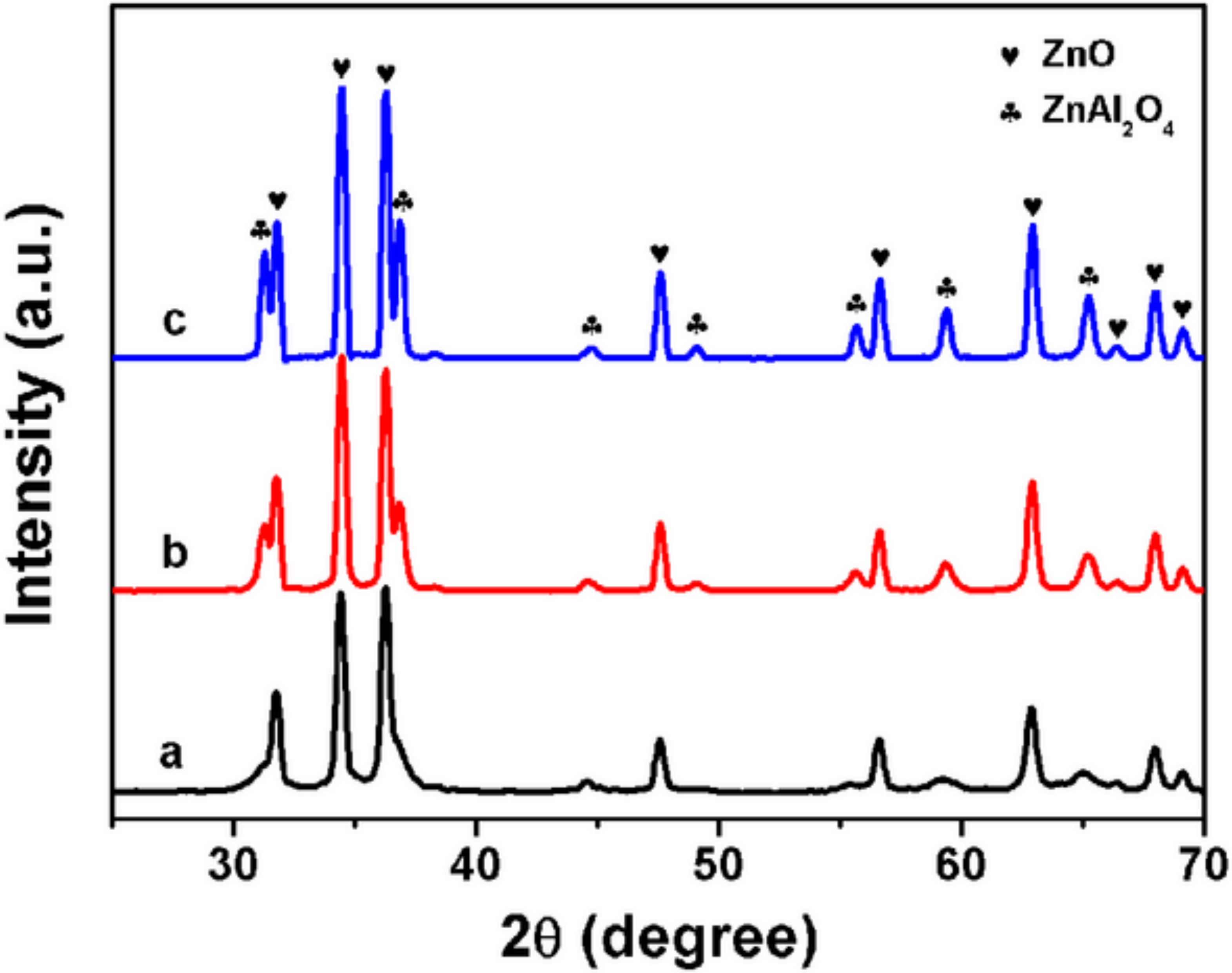

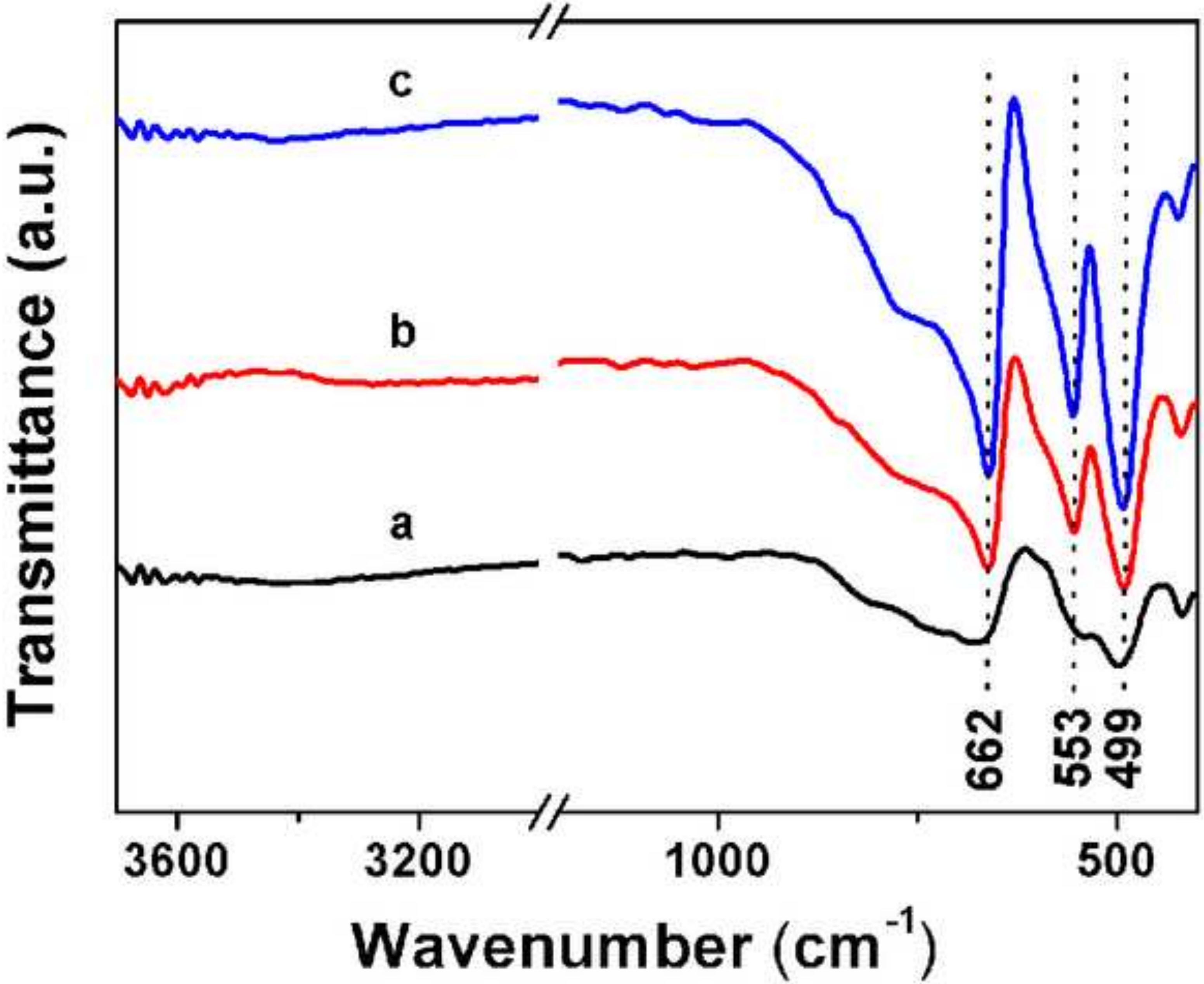
c
b
a
662
553
499
3600
3200
1000
500
Transmittance (a.u.)
Wavenumber (cm^{-1})

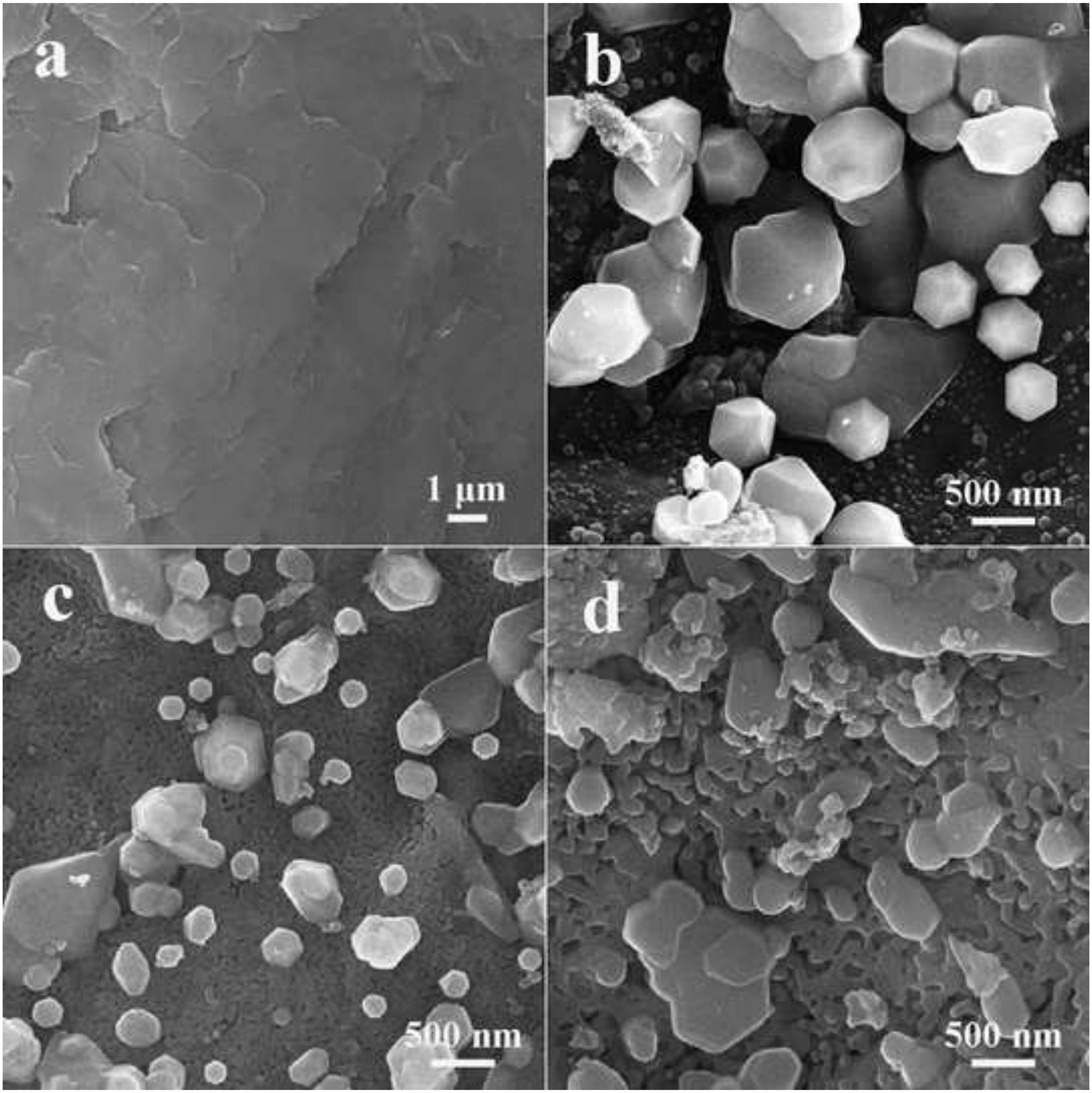
a
1 µm
b
500 nm
c
500 nm
d
500 nm

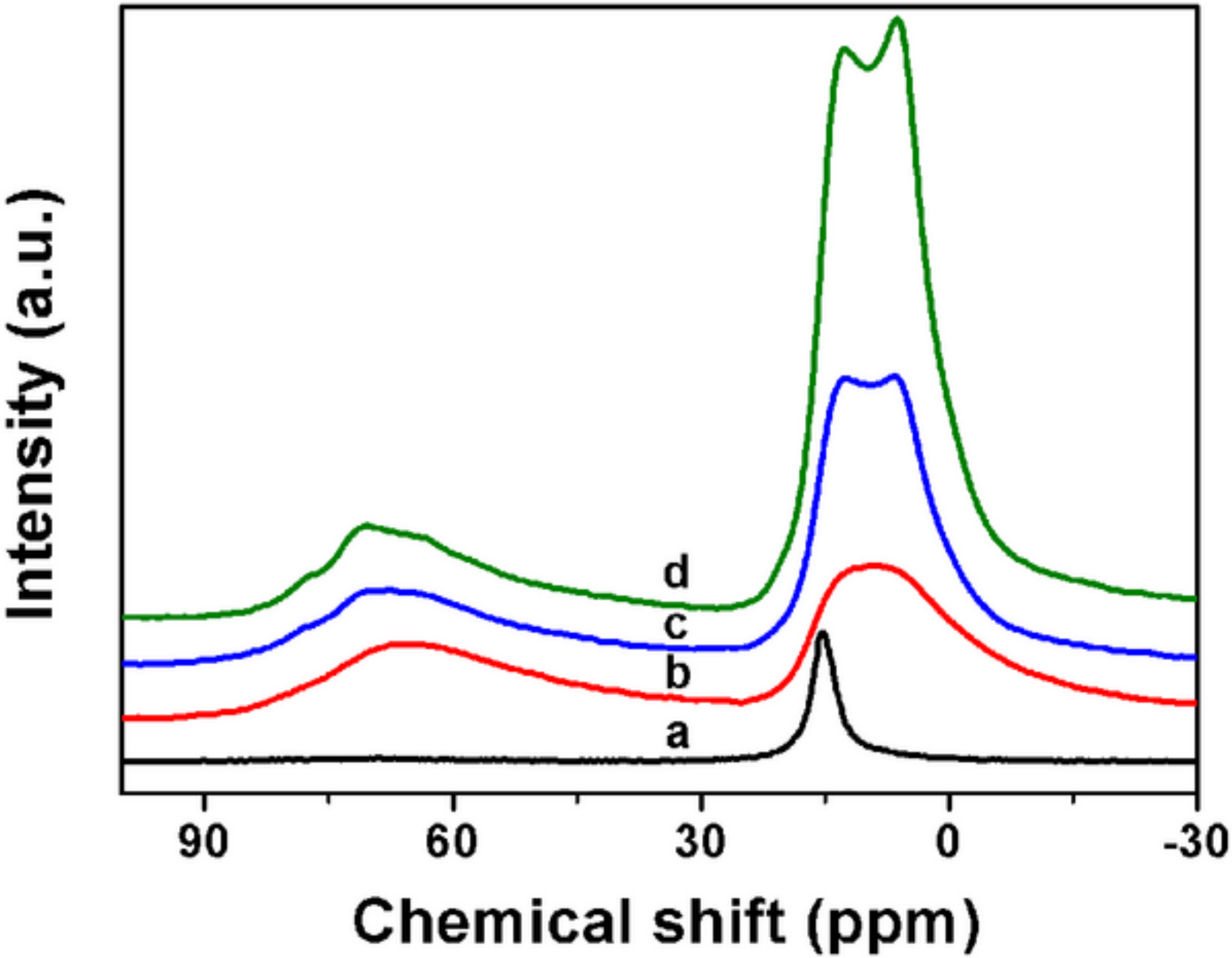
Intensity (a.u.)
d
c
b
a
90
60
30
0
-30
Chemical shift (ppm)

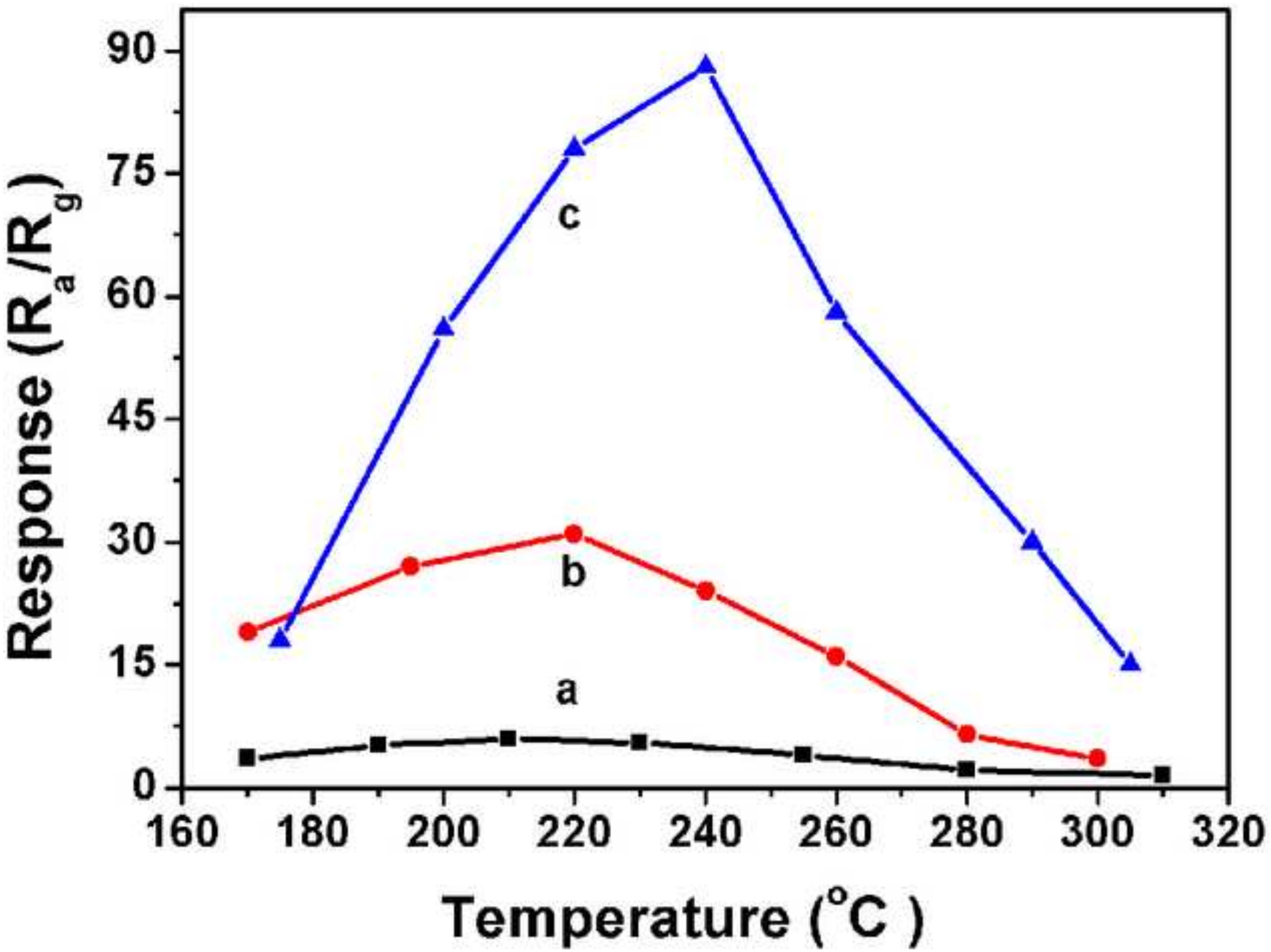

Response (R_a/R_g)
90
75
60
45
30
15
0
c
b
a
160
180
200
220
240
260
280
300
320
Temperature (°C)

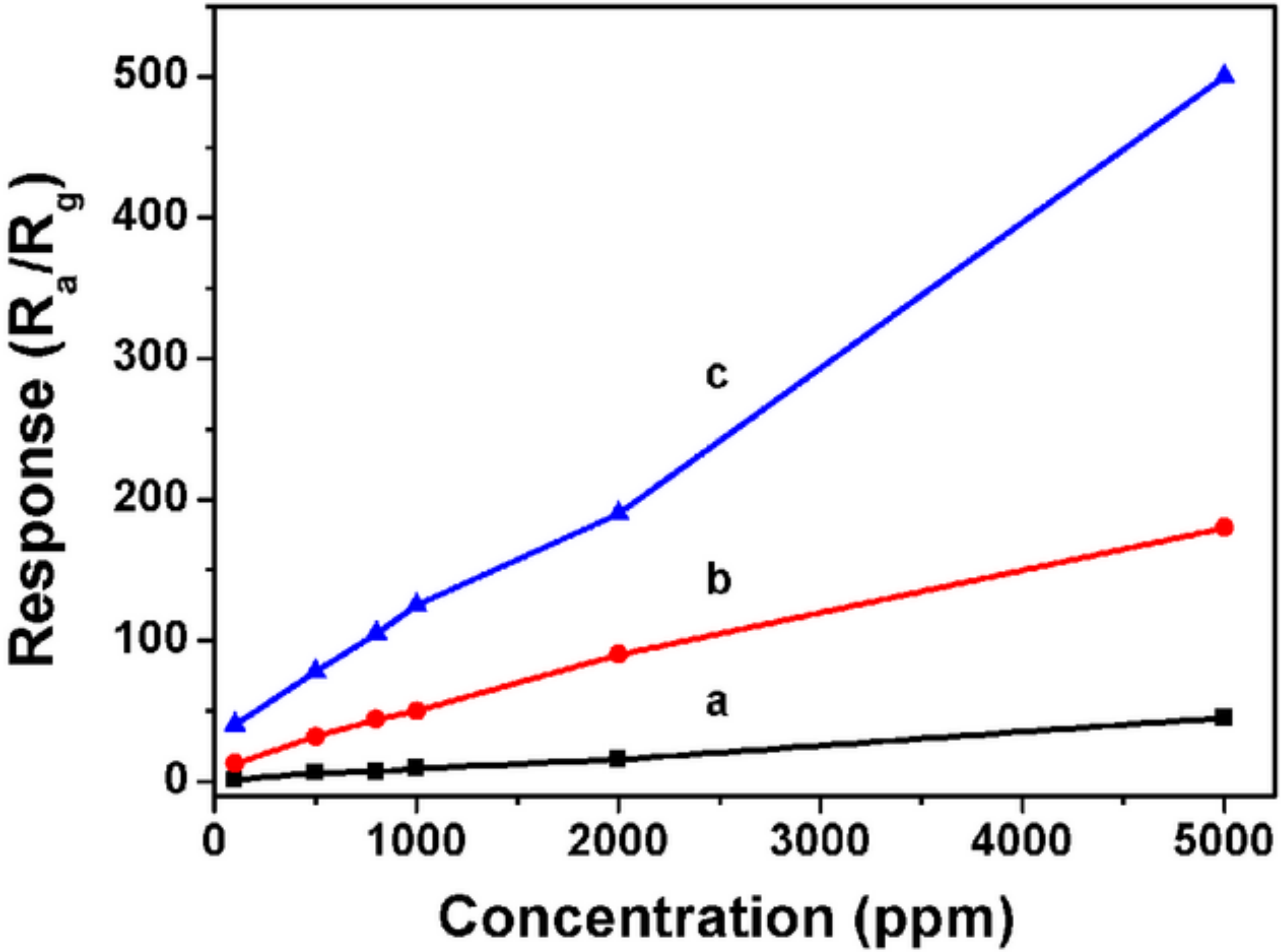
Response (R_a/R_g)
0
100
200
300
400
500
Concentration (ppm)
0
1000
2000
3000
4000
5000
a
b
c

Figure(s)

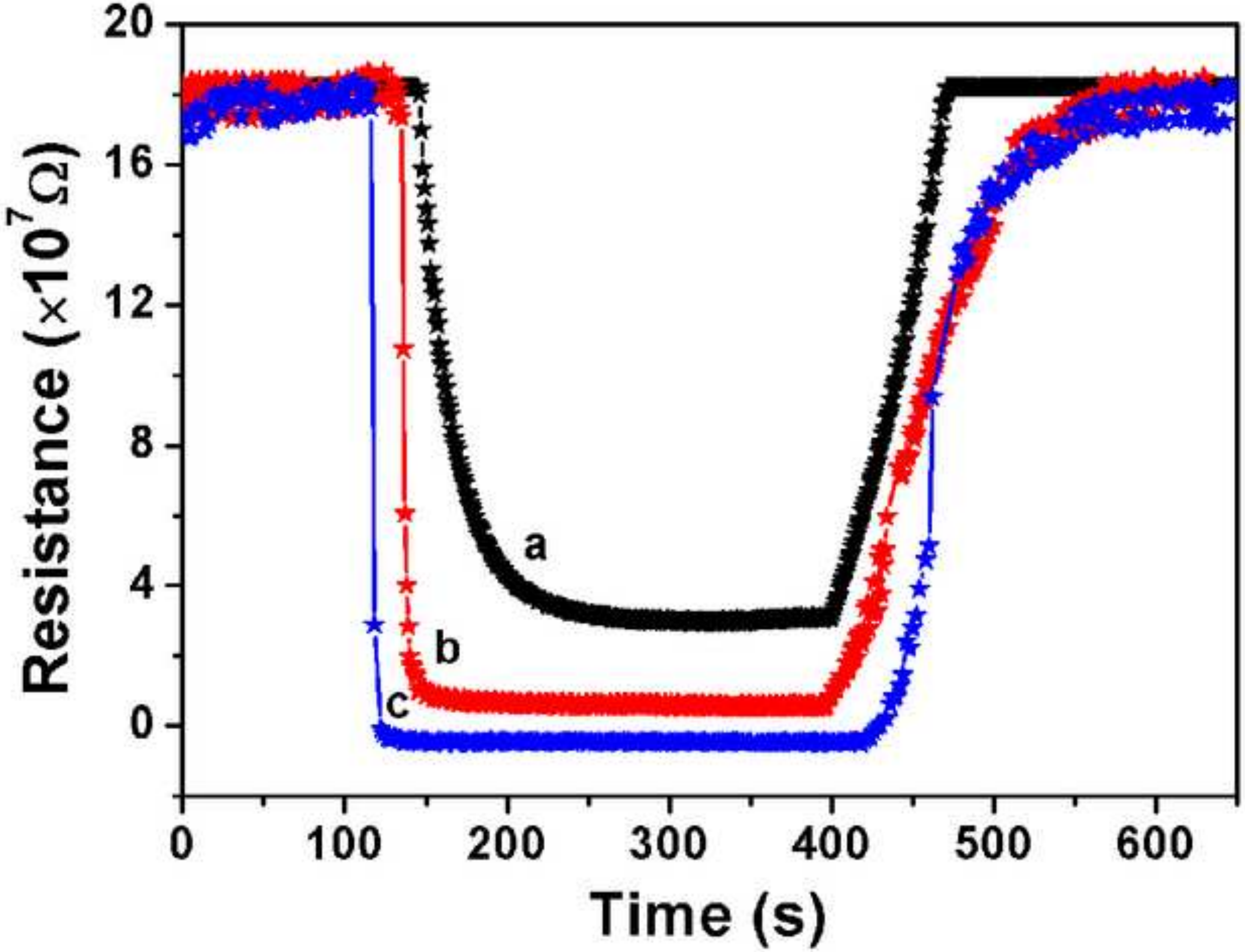

20
16
12
8
4
0
Resistance (×10^{7}Ω)
0
100
200
300
400
500
600
Time (s)
a
b
c

Figure(s)

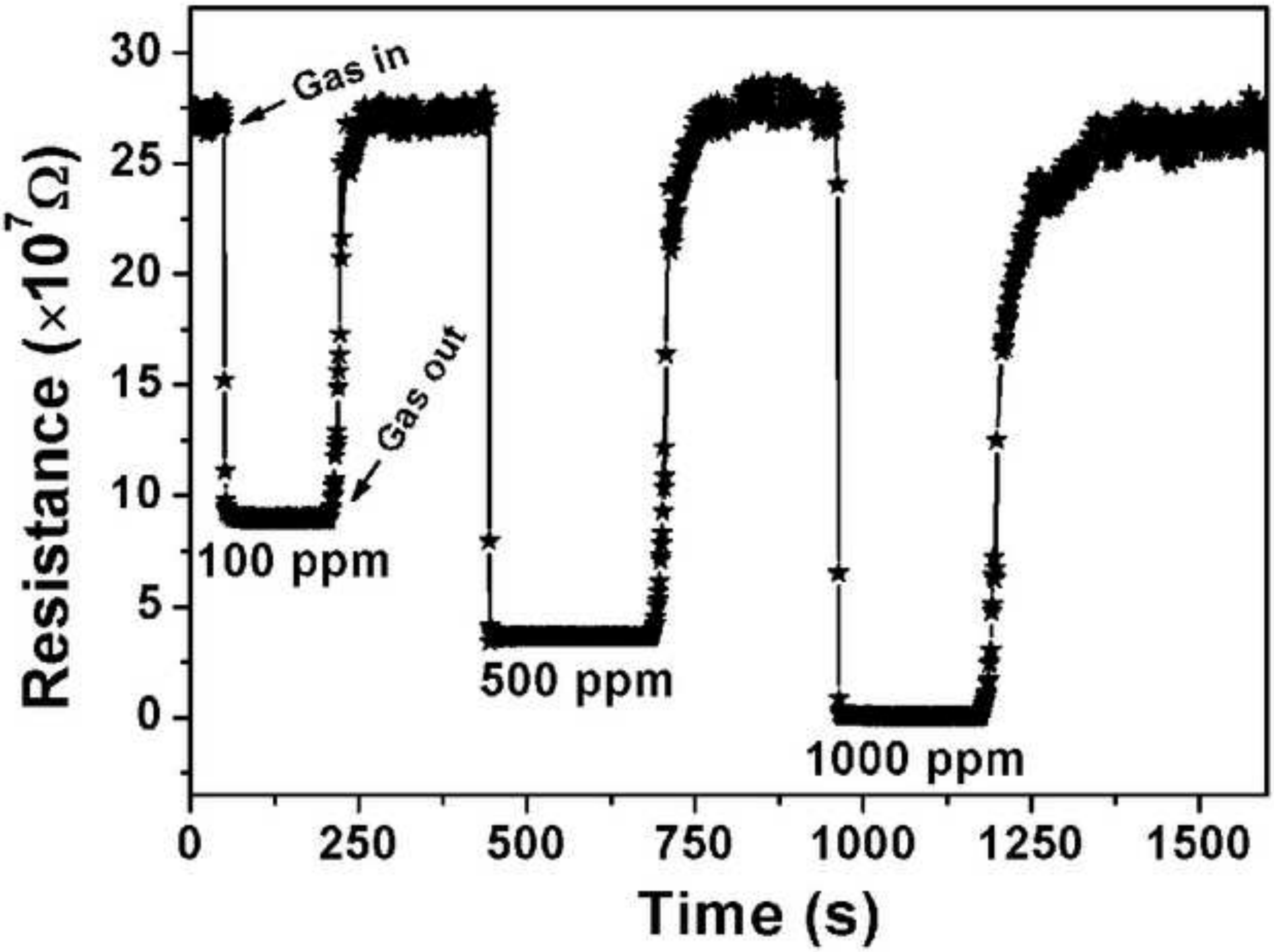

Resistance (×10^7 Ω)
30
25
20
15
10
5
0
Gas in
Gas out
100 ppm
500 ppm
1000 ppm
0
250
500
750
1000
1250
1500
Time (s)

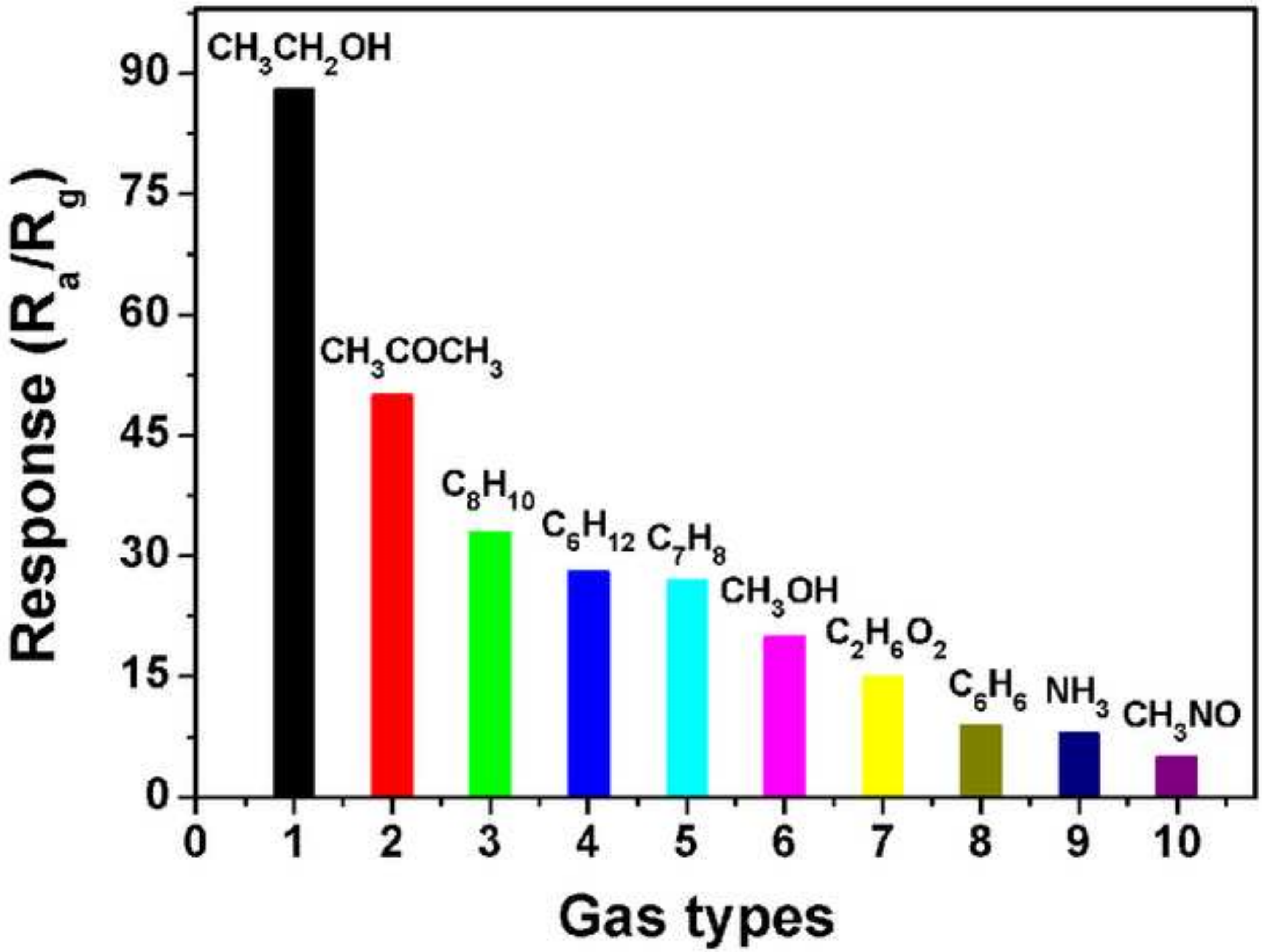
Response (R_a/R_g)
Gas types
0
15
30
45
60
75
90
0
1
2
3
4
5
6
7
8
9
10
CH_3CH_2OH
CH_3COCH_3
C_8H_{10}
C_6H_{12}
C_7H_8
CH_3OH
$C_2H_6O_2$
C_6H_6
NH_3
CH_3NO

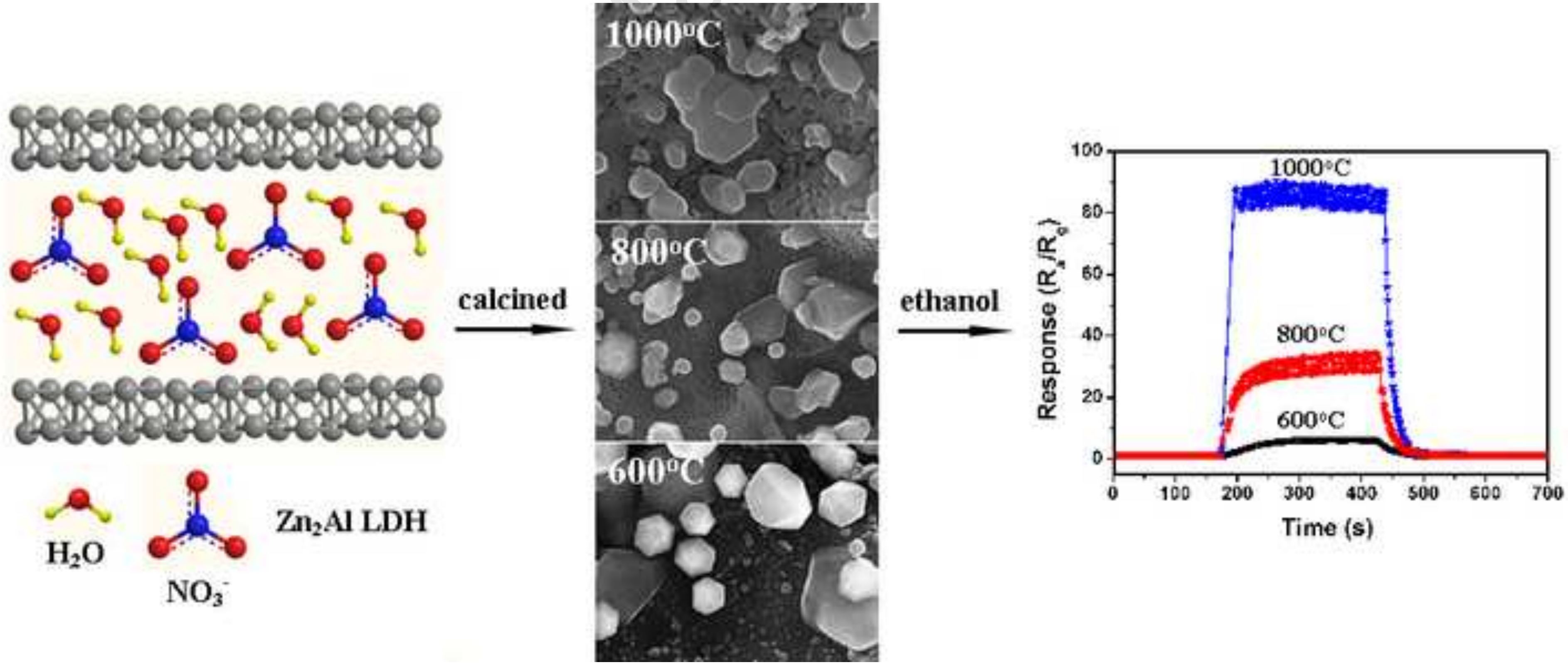
H$_2$O
NO$_3^-$
Zn$_2$Al LDH
calcined
1000°C
800°C
600°C
ethanol
Response (R$_a$/R$_g$)
Time (s)
0
20
40
60
80
100
0
100
200
300
400
500
600
700
1000°C
800°C
600°C